

**000 A slow-releasing form of prostacyclin agonist (ONO1301SR) enhances endogenous secretion of multiple cardiotherapeutic cytokines and improves cardiac function in a rapid-pacing-induced model of canine heart failure**

*Tomonori Shirasaka, MD, Shigeru Miyagawa, MD, PhD, Satsuki Fukushima, MD, PhD, Atsuhiko Saito, PhD, Motoko Shiozaki, PhD, Naomasa Kawaguchi, PhD, Nariaki Matsuura, MD, PhD, Satoshi Nakatani, MD, PhD, Yoshiki Sakai, PhD, Takashi Daimon, PhD, Yutaka Okita, MD, PhD, and Yoshiki Sawa, MD, PhD, Kobe, Suita, Osaka, and Hyogo, Japan*

In vitro, ONO1301, a prostacyclin agonist, enhances secretion of multiple cardiotherapeutic cytokines. In vivo, Intramyocardial administration of ONO1301SR, a slow-releasing form of ONO1301, attenuated the cardiac function in the canine DCM heart failure model. Especially, region specific effects of ONO1301SR were proved by speckle tracking echocardiography and histopathological study.

## Treatment of cerebral ischemia-reperfusion injury with PEGylated liposomes encapsulating FK506

Takayuki Ishii,\* Tomohiro Asai,\* Dai Oyama,\* Yurika Agato,\* Nodoka Yasuda,\* Tatsuya Fukuta,\* Kosuke Shimizu,\* Tetsuo Minamino,<sup>†</sup> and Naoto Oku\*<sup>1</sup>

\*Department of Medical Biochemistry, School of Pharmaceutical Sciences, University of Shizuoka, Shizuoka, Japan; and <sup>†</sup>Department of Cardiovascular Medicine, Osaka University Graduate School of Medicine, Osaka, Japan

**ABSTRACT** FK506 (Tacrolimus) has the potential to decrease cerebral ischemia-reperfusion injury. However, the clinical trial of FK506 as a neuroprotectant failed due to adverse side effects. This present study aimed to conduct the selective delivery of FK506 to damaged regions, while at the same time reducing the dosage of FK506, by using a liposomal drug delivery system. First, the cytoprotective effect of polyethylene glycol-modified liposomes encapsulating FK506 (FK506-liposomes) on neuron-like pheochromocytoma PC12 cells was examined. FK506-liposomes protected these cells from H<sub>2</sub>O<sub>2</sub>-induced toxicity in a dose-dependent manner. Next, we investigated the usefulness of FK506-liposomes in transient middle cerebral artery occlusion (t-MCAO) rats. FK506-liposomes accumulated in the brain parenchyma by passing through the disrupted blood-brain barrier at an early stage after reperfusion had been initiated. Histological analysis showed that FK506-liposomes strongly suppressed neutrophil invasion and apoptotic cell death, events that lead to a poor stroke outcome. Corresponding to these results, a single injection of FK506-liposomes at a low dosage significantly reduced cerebral cell death and ameliorated motor function deficits in t-MCAO rats. These results suggest that liposomalization of FK506 could reduce the administration dose by enhancing the therapeutic efficacy; hence, FK506-liposomes should be a promising neuroprotectant after cerebral stroke.—Ishii, T., Asai, T., Oyama, D., Agato, Y., Yasuda, N., Fukuta, T., Shimizu, K., Minamino, T., Oku, N. Treatment of cerebral ischemia-reperfusion injury with PEGylated

liposomes encapsulating FK506. *FASEB J.* 27, 1362–1370 (2013). [www.fasebj.org](http://www.fasebj.org)

*Key Words:* neuroprotectant • tacrolimus • apoptosis • inflammation • motor function

AFTER RESTORATION OF BLOOD FLOW in cerebral stroke patients, cerebral ischemia-reperfusion (I/R) injury often occurs, resulting in neurological deficits (1, 2). Hence, the development of neuroprotective therapy for this type of injury has been awaited for a better outcome after a cerebral stroke. Although >1000 candidate compounds have shown potency as a neuroprotectant, and >100 of them have been tested in clinical studies in the past, none of them have passed these trials due to insufficiency of medicinal efficacy and to adverse side effects (3, 4). To overcome the present situation, we previously applied the liposomal drug delivery system (DDS) to the treatment of cerebral I/R injury (5). When 100 nm liposomes were intravenously injected immediately after the start of reperfusion, they selectively accumulated in the I/R region, suggesting that drug delivery using liposomes is applicable for treatment of I/R injuries. Moreover, liposomes modified with the antiapoptotic protein asialoerythropoietin significantly suppressed cerebral cell death and improved motor functional deficits induced by I/R injury in transient middle cerebral artery occlusion (t-MCAO) rats by increasing the accumulation of the protein in the injured region compared with the outcome for the free asialoerythropoietin-treated group. This finding offers the possibility that liposomal DDS could be a useful strategy for the treatment of cerebral I/R injury. However, the efficacy of liposomal DDS for treatment of cerebral I/R injuries has been proven for just a single protein, *i.e.*, asialoerythropoietin. Accordingly, more study is needed to reinforce the utility of this therapeutic

Abbreviations: DDS, drug delivery system; DiI-C<sub>18</sub>, 1,1'-dioctadecyl-3,3,3',3'-tetramethylindocarbocyanine; DPPC, dipalmitoylphosphatidylcholine; DSPE, distearoylphosphatidylethanolamine; FK506-liposome, polyethylene glycol-modified liposomes encapsulating FK506; HCO-60, polyoxyethylene (60) hydrogenated castor oil; HS, horse serum; ICA, internal carotid artery; I/R, ischemia-reperfusion; IVIS, *in vivo* imaging system; MCA, middle cerebral artery; MPO, myeloperoxidase; NGF, nerve growth factor; PEG, polyethylene glycol; t-MCAO, transient middle cerebral artery occlusion; TTC, 2,3,5-triphenyltetrazolium chloride; TTW, therapeutic time window; TUNEL, terminal deoxyribonucleotidyl transferase (TDT)-mediated dUTP-digoxigenin nick end labeling

<sup>1</sup> Correspondence: Department of Medical Biochemistry, School of Pharmaceutical Sciences, University of Shizuoka, 52-1 Yada, Suruga-ku, Shizuoka 422-8526, Japan. E-mail: [oku@u-shizuoka-ken.ac.jp](mailto:oku@u-shizuoka-ken.ac.jp)  
doi: 10.1096/fj.12-221325

This article includes supplemental data. Please visit <http://www.fasebj.org> to obtain this information.

tic strategy. The therapeutic effect of liposomes encapsulating a neuroprotective chemodrug on I/R injury has not been examined yet. Therefore, in this study designed for achieving this purpose and developing a novel neuroprotectant, we prepared polyethylene glycol (PEG)-modified liposomes encapsulating FK506 (FK506-liposomes).

The immunosuppressant FK506 has been widely used to prevent allograft rejections in clinical organ transplantation, and was also recently reported to be a drug candidate for the treatment of acute stroke in animal studies (6–8). Calcineurin is activated by excessive influx of  $\text{Ca}^{2+}$  into cerebral cells after a cerebral ischemic event, resulting in the induction of nitric oxide, generation of inflammatory cytokines, and the release of cytochrome *c* (9–12). FK506 inhibits the activation of calcineurin by associating with the FK506-binding protein (FKBP) in neuronal cells and glial cells; hence, it shows a neuroprotective effect on experimental stroke models. However, the frequent administration of FK506 required to achieve a good outcome has the risk of developing side effects such as heart deficits and nephrotoxicity. The liposomalization of FK506 is a promising approach for changing the bio-distribution and negating the problem of poor water solubility (13, 14). The liposomal formulation of FK506 is as effective as an equal dose of commercial FK506 in preventing the rejection of transplant grafts, but with considerably less nephrotoxicity (14). The efficient delivery of FK506 to ischemic regions by using liposomes might potentially reduce the administration dosage without changing neuroprotective efficacy. In the present study, we assessed the potential of FK506-liposomes as a neuroprotectant against cerebral I/R injury by investigating their cerebral distribution, pharmacological activity, therapeutic effect, and therapeutic time window in t-MCAO rats.

## MATERIALS AND METHODS

### Animals

Male Wistar rats (170–210 g) were purchased from Japan SLC, Inc. (Shizuoka, Japan). The animals were cared for according to the Animal Facility Guidelines of the University of Shizuoka. All animal procedures were approved by the Animal and Ethics Review Committee of the University of Shizuoka.

### Preparation of FK506-liposomes

The lipid composition of FK506-liposomes was dipalmitoylphosphatidylcholine (DPPC) and distearoylphosphatidylethanolamine (DSPE)-PEG (molecular weight of PEG was 2000) in a 20:1 molar ratio. FK506-liposomes were prepared by the following freeze-drying method: FK506 was dissolved in methanol and added to a flask containing the above lipids dissolved in *tert*-butylalcohol. The molar ratio of FK506 to DPPC was 1:50. The solution was lyophilized, and then the lyophilizate was hydrated with PBS (pH 7.4) at 50°C. The liposome solution was freeze-thawed for 3 cycles with liquid nitrogen. Then the particle size of the liposomes was adjusted by

extrusion through 100-nm pore-size polycarbonate filters (Nuclepore, Cambridge, MA, USA). Unencapsulated FK506 was removed by ultracentrifugation at 604,000 *g* for 15 min (Hitachi, Tokyo, Japan), and the concentration of FK506 in the liposomes was determined by HPLC (Hitachi). Final liposomal concentration was 10 mM as DSPC. FK506-liposomes were dissolved in tetrahydrofuran, and 20  $\mu\text{l}$  of the solution was injected into an octadecylsilane (ODS) column (TSK gel ODS-80TM, 4.6 $\times$ 150 mm, Tosoh, Tokyo, Japan). The mobile phase consisted of acetonitrile and water (3:2, v/v). HPLC analysis was performed at 60°C and a flow rate of 1 ml/min with UV detection at 214 nm. For the cerebral distribution study, 1,1'-dioctadecyl-3,3,3',3'-tetramethylindocarbocyanine (DiI-C<sub>18</sub>; Molecular Probes Inc., Eugene, OR, USA) was mixed with the initial lipid solution for fluorescence labeling of the liposomes.

### Cell culture

Pheochromocytoma cells [PC12 cells; European Collection of Cell Cultures (ECACC), Porton Down, UK] were cultured in high-glucose DME medium (Wako, Osaka, Japan) supplemented with streptomycin (100  $\mu\text{g}/\text{ml}$ ), penicillin (100 U/ml), heat-inactivated 5% fetal bovine serum (FBS; Japan Bioserum, Tokyo, Japan), and 10% horse serum (HS; MP Biomedicals, Solon, OH, USA) at 37°C in a humidified chamber with 5%  $\text{CO}_2$ . PC12 cells were plated on poly-D-lysine-coated 24-well plates for the WST (viability) assay. These cells were caused to differentiate into nerve-like cells by adding nerve growth factor (NGF) at 100 ng/ml to DME medium containing 0.5% HS. Five days after incubation with NGF, these cells were used for subsequent experiments.

### Cell proliferation assays

FK506-liposomes (0.01, 0.1, or 1.0  $\mu\text{M}$  as FK506 dosage) or free FK506 (1.0  $\mu\text{M}$ ) were added to differentiated PC12 cells in 24-well plates.  $\text{H}_2\text{O}_2$  was added to each well to a final concentration of 75  $\mu\text{M}$  at 30 min after addition of the samples. The number of viable cells was measured by using TetraColor One (Seikagaku, Tokyo, Japan). Briefly, TetraColor One solution was added to each well, and the cells were then incubated at 37°C for 3 h in a humidified atmosphere containing 5%  $\text{CO}_2$ . Absorbance at 450 nm was measured by using a Tecan Infinite M200 microplate reader (Tecan, Männedorf, Switzerland). FK506 was dissolved in ethanol, and the final concentration of ethanol was 0.1% in medium.

### t-MCAO rats

Preparation of t-MCAO rats was performed as described previously (15). Briefly, anesthesia was induced with 3% isoflurane and maintained with 1.5% isoflurane during surgery. During surgery, the body temperature of the rats was maintained at 37°C with a heating pad. After a median incision of the neck skin had been made, the right carotid artery, external carotid artery, and internal carotid artery (ICA) were isolated with careful conservation of the vagal nerve. An  $\sim$ 18 mm 4-0 monofilament nylon suture coated with silicon was introduced into the right ICA and advanced to the origin of the MCA to occlude it. Silk thread was used for ligation to keep the filament at the site of insertion into the MCA. After the surgery, the neck was closed; anesthesia was then discontinued. MCAO was performed for 1 h. Success of the surgery was judged by the appearance of hemiparesis and an increase in body temperature ( $>37.8^\circ\text{C}$ ). Reperfusion was started by withdrawing the filament  $\sim$ 10 mm at 1 h after the start of occlusion under isoflurane anesthesia.

## Drug administration

Polyoxyethylene (60) hydrogenated castor oil (HCO-60; 200 mg/ml), including 10% ethanol was used as vehicle for free FK506. FK506 or FK506-liposomes were intravenously injected at a single dose of 30, 100, or 300  $\mu\text{g}/\text{kg}$  body weight (0.5 ml/rat) immediately after the start of reperfusion. In the therapeutic time window study, the injection time was shifted as indicated in the legend of Fig. 6. It was reported earlier that the vehicle has no effect on the outcome of ischemia (6, 16, 17).

## Cerebral distribution of FK506-liposomes

PEGylated liposomes and FK506-liposomes were fluorescently labeled with DiI-C<sub>18</sub> as described above. They were intravenously injected into the t-MCAO rats at the start of reperfusion. The rats were euthanized at 3 or 24 h after the injection, and their brains were sliced into 2-mm-thick coronal sections with a rat brain slicer (Muromachi Kikai, Tokyo, Japan). All sections were put on glass slides, and the fluorescence of DiI was measured with an *in vivo* imaging system (IVIS; Xenogen Corp., Alameda, CA, USA). Thereafter, these sections were embedded in optical cutting temperature (OCT) compound (Sakura, Finetech., CO Ltd., Tokyo, Japan) and then frozen in a dry ice/ethanol bath. These frozen sections were cut into 10- $\mu\text{m}$  ones with a cryostat (HM505E; Microm, Walldorf, Germany) for subsequent immunostaining experiments. Average photon counts in I/R region were calculated from 4 rats at each time.

## Immunostaining for CD31

The sections were incubated with 1% bovine serum albumin in PBS for 10 min at room temperature for blocking, and then with biotinylated anti-mouse CD31 rat monoclonal antibody (BD Pharmingen, Franklin Lakes, NJ, USA) for 18 h at 4°C, and thereafter with streptavidin-Alexa fluor 488 conjugates (Molecular Probes Inc.) for 30 min at room temperature. Finally, the sections were mounted with Perma Fluor Aqueous Mounting Medium (Thermo Shandon, Pittsburgh, PA, USA) and observed for fluorescence in the striatum with an LSM microscope system (Carl Zeiss Co., Ltd., Oberkochen, Germany).

## Terminal deoxyribonucleotidyl transferase (TDT)-mediated dUTP-digoxigenin nick end labeling (TUNEL) staining

Brains of t-MCAO rats were dissected at 24 h after the injection of FK506-liposomes (100  $\mu\text{g}/\text{kg}$  as FK506 dosage), free FK506 (100  $\mu\text{g}/\text{kg}$ ), PEGylated liposomes (same lipid concentration as FK506-liposomes), or PBS; embedded in optimal cutting temperature (OCT) compound (Sakura Finetek, Torrance, CA, USA); and then frozen in dry ice/ethanol. Frozen sections (10  $\mu\text{m}$ ) were prepared by using a cryostatic microtome (HM 505E, Microm, Walldorf, Germany) and were stained with TUNEL reagents supplied in an ApopTag Plus fluorescein *in situ* apoptosis detection kit (Chemicon International, Inc., Temecula, CA, USA), as described below. For fixation of the sections, they were incubated in 4% paraformaldehyde for 15 min at room temperature, and then in ethanol/acetic acid (2:1) solution for 5 min at  $-20^\circ\text{C}$ . DNA strand breaks were labeled with the digoxigenin-conjugated terminal deoxynucleotidyl transferase enzyme by incubation for 1 h at  $37^\circ\text{C}$ . Then, the sections were incubated in antidigoxigenin-fluorescein solution for 30 min at room temperature. Finally, the sections were mounted with Perma Fluor aqueous mounting medium including DAPI (1.0  $\mu\text{g}/\text{ml}$ ) and observed for fluorescence with the LSM system.

The observed area in the striatum was similar to the imaged region in Fig. 2C, D. For quantitative evaluation, the number of TUNEL-positive cells was counted in 4 sections/rat. Five rats were used to obtain the quantitative data.

## Histological analysis of neutrophil influx

Frozen sections (7  $\mu\text{m}$ ) were prepared as described above. For fixation of these sections, they were incubated in acetone for 1 min at room temperature, and then in 0.3% H<sub>2</sub>O<sub>2</sub> solution for 30 min at room temperature. After having been blocked with fetal bovine serum for 20 min at room temperature, the sections were incubated with anti-myeloperoxidase (MPO) rabbit polyclonal antibody (Thermo Fisher Scientific, Rockford, IL, USA) for 30 min at room temperature. A Vectastain ABC rabbit IgG kit and DAB peroxidase substrate kit (both from Vector Laboratories, Inc., Burlingame, CA, USA) were used for identification of neutrophils in the sections. Finally, the sections were counterstained with hematoxylin and observed microscopically (BX51; Olympus, Tokyo, Japan). The observed area in the striatum was similar to the imaged region in Fig. 2C, D.

## Therapeutic experiment

FK506-liposomes (30 or 100  $\mu\text{g}/\text{kg}$  as FK506 dosage), PBS, free FK506 (30, 100, or 300  $\mu\text{g}/\text{kg}$ ), or vehicle (200 mg/ml HCO-60 including 10% ethanol in PBS) for FK506 were intravenously injected into t-MCAO rats immediately after the start of reperfusion. The volume of damaged region, the degree of brain swelling, and the functional outcome of rats were assessed at 24 h after the injection. For the functional outcome study, the rats underwent a 21-point neurological score analysis prior to sacrifice, as described previously (18). All of the normal and sham-operated rats received 21 points in this test. After this study, the brains of t-MCAO rats were sliced into 2-mm-thick coronal sections by using a rat brain slicer (Muromachi Kikai) and stained with 2,3,5-triphenyltetrazolium chloride (TTC; Wako) for the detection of cerebral cell death. The volume of the damaged regions was calculated by using an image-analysis system (Image J; U.S. National Institutes of Health, Bethesda, MD, USA). The damaged regions were considered to be those appearing completely white. Brain swelling was calculated as the ratio of volumes between ipsilateral and contralateral hemisphere sections.

## Assessment of therapeutic time window

t-MCAO rats were intravenously injected with FK506-liposomes (30 or 100  $\mu\text{g}/\text{kg}$  as FK506 dosage) or PBS at various times after the start of reperfusion. The volume of damaged regions was assessed at 24 h after injection by using TTC staining as described above.

## Statistical analysis

Statistical analysis was performed by 1-way analysis of variance (ANOVA) followed by Dunnett's multiple comparison tests. Data are presented as means  $\pm$  SD.

## RESULTS

### FK506-liposomes protected differentiated PC12 cells from H<sub>2</sub>O<sub>2</sub>-induced toxicity

The particle size and  $\zeta$ -potential of FK506 liposomes were  $109 \pm 4.3$  nm and  $-7.2 \pm 0.7$  mV, respectively. To

assess the pharmacological activity of FK506-liposomes, we examined the cytoprotective effect of them on differentiated PC12 cells treated with H<sub>2</sub>O<sub>2</sub>. The number of live PC12 cells was decreased to ~40% by exposure to H<sub>2</sub>O<sub>2</sub> (Fig. 1). FK506-liposomes suppressed this cell death induced by H<sub>2</sub>O<sub>2</sub> in a dose-dependent manner, whereas empty-liposomes (PEGylated liposomes) showed no cytoprotective effect against the H<sub>2</sub>O<sub>2</sub>-induced toxicity.

### FK506-liposomes diffused into the brain parenchyma only in the ischemic hemisphere

The intracerebral distribution of FK506-liposomes given immediately after the start of reperfusion to t-MCAO rats was observed at 3 h (Fig. 2A) and 24 h (Fig. 2B) after the injection. The fluorescence of DiI-labeled FK506-liposomes was observed only in the ischemic hemisphere at both time points. Immunohistological analysis revealed that the FK506-liposomes had leaked into the brain parenchyma from cerebral vessels in the ipsilateral hemisphere (Fig. 2C, D). Moreover, higher DiI fluorescence intensity was detected in the brain sections prepared at 24 h after the injection than in those prepared at 3 h (Fig. 2E) after it, which suggests that the accumulation of FK506-liposomes in the brain parenchyma gradually increased by continuous leakage from cerebral vessels according to enhanced permeability and the retention effect. In contrast, no leakage of them into the cerebral parenchyma of the contralateral hemisphere occurred.

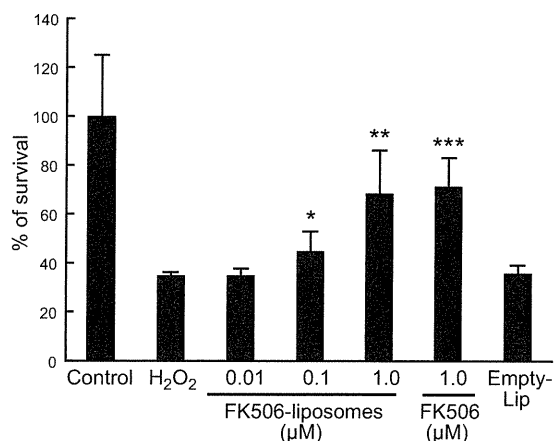


**Figure 1.** FK506-liposome-mediated attenuation of H<sub>2</sub>O<sub>2</sub>-induced cytotoxicity toward differentiated PC12 cells. PC12 cells were caused to differentiate by the addition of NGF at 100 ng/ml to culture medium supplemented with 0.5% HS. After 5 d in culture for differentiation, FK506-liposomes, free FK506, or empty liposomes (Empty-Lip) were added to the culture medium, and then H<sub>2</sub>O<sub>2</sub> was added to each well. After 24 h, viable cell numbers were determined by performing the WST assay. Final lipid concentration of empty liposomes was same as that of FK506-liposomes. Data are presented as means ± SD (*n*=6). \**P* < 0.05, \*\**P* < 0.01, \*\*\**P* < 0.001 vs. H<sub>2</sub>O<sub>2</sub>-treated group.

### FK506-liposomes showed antiapoptotic effect in t-MCAO rats

At 24 h after the injection of each sample, apoptosis of the cerebral cells in t-MCAO rats was identified by TUNEL staining (Fig. 3). TUNEL-positive cells were detected in neither the striatum nor the cerebral cortex in the nonischemic hemisphere (data not shown). A number of apoptotic cells were observed in the control group and free FK506-treated group (Fig. 3A, B). This dosage (100 μg/kg) of free FK506 was too low to exert an antiapoptotic effect in t-MCAO rats. However, FK506-liposomes obviously reduced the number of TUNEL-positive cells despite the same dosage as free FK506. Quantitative analysis of TUNEL-positive cells elucidated the difference between each group (Fig. 3C). In the FK506-liposome-treated group, the number of apoptotic cells in the striatum was significantly reduced compared with that in the other groups. In contrast to this result, there was no significant difference in the cortex between FK506-liposome-treated group and other groups, even though this treatment tended to suppress the cerebral apoptosis. Empty liposomes had no effect on apoptosis induced by I/R injury.

### FK506-liposomes suppressed neutrophil invasion induced by I/R

To evaluate anti-inflammatory effect of FK506-liposomes, we examined neutrophil invasion into I/R regions as an indicator of intracerebral inflammation (Fig. 4). In the nonischemic hemisphere of all groups, almost no MPO-stained cells were identified (data not shown). Conversely, a number of neutrophils that had infiltrated were detected in the striatum and the cortex of the ischemic hemisphere (Fig. 4A, control). In the FK506-liposome-treated group, few MPO-positive cells were observed in the striatum, whereas they were more numerous in the cortex. The quantitative analysis revealed that FK506-liposomes reduced the number of infiltrating neutrophils in the striatum by ~80%, and significantly suppressed neutrophil invasion compared with the treatment with the same dosage of free FK506 (Fig. 4B).

### FK506-liposomes ameliorated cerebral I/R injury in t-MCAO rats

t-MCAO caused cerebral cell death and brain swelling in these experimental model rats. Treatment with free FK506 at 30 or 100 μg/kg hardly affected the damaged region and brain swelling induced by I/R, whereas FK506-liposomes at these same dosages as the free drug significantly reduced the amount of brain damage (Fig. 5A, B). Furthermore, administration of FK506-liposomes at 100 μg/kg showed therapeutic efficacy quite similar to that obtained with the free drug at 300 μg/kg. These results suggest that liposomalization of FK506 enhanced its cytoprotective



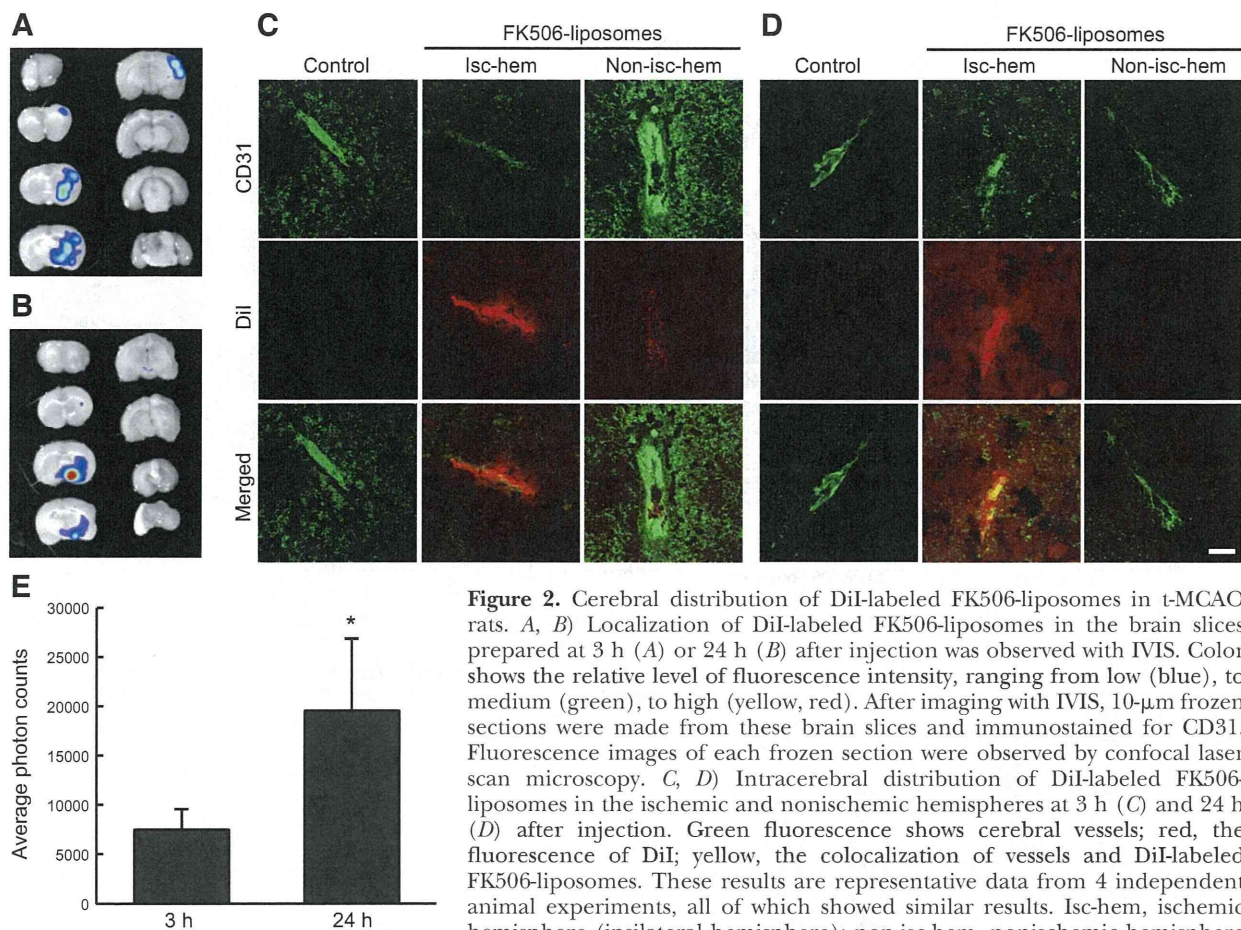


**Figure 2.** Cerebral distribution of DiI-labeled FK506-liposomes in t-MCAO rats. *A, B*) Localization of DiI-labeled FK506-liposomes in the brain slices prepared at 3 h (*A*) or 24 h (*B*) after injection was observed with IVIS. Color shows the relative level of fluorescence intensity, ranging from low (blue), to medium (green), to high (yellow, red). After imaging with IVIS, 10- $\mu$ m frozen sections were made from these brain slices and immunostained for CD31. Fluorescence images of each frozen section were observed by confocal laser scan microscopy. *C, D*) Intracerebral distribution of DiI-labeled FK506-liposomes in the ischemic and nonischemic hemispheres at 3 h (*C*) and 24 h (*D*) after injection. Green fluorescence shows cerebral vessels; red, the fluorescence of DiI; yellow, the colocalization of vessels and DiI-labeled FK506-liposomes. These results are representative data from 4 independent animal experiments, all of which showed similar results. Isc-hem, ischemic hemisphere (ipsilateral hemisphere); non-isc-hem, nonischemic hemisphere (contralateral hemisphere). Scale bar = 20  $\mu$ m. *E*) Average photon counts in the ischemic hemisphere were determined by the image of brain slices with IVIS ( $n=4$ ). \* $P < 0.05$ .

effect due to improved biodistribution. In accordance with several reports, the extent of cerebral cell death, as indicated by reduced brain volume (Fig. 5A), and that of brain swelling (Fig. 5B) were similar in both control (PBS-injected) and vehicle-injected groups.

The therapeutic time window (TTW) of agents is critical information for developing neuroprotectants, particularly in designing the clinical trial. The TTW of FK506-liposomes was estimated by altering the time of injection after the commencement of reperfusion (Fig. 6). The volume of brain damage in the t-MCAO rats was significantly decreased by the dose of FK506-liposomes administered at 30  $\mu$ g/kg as FK506 up through 2 h after reperfusion had begun. However, the treatment with the same dose of FK506-liposomes given at 3 h after the start of reperfusion or later had almost no effect on cerebral cell death, as judged by the results of TTC staining. Moreover, a higher amount of FK506-liposomes (100  $\mu$ g/kg as FK506) injected at 3 h after reperfusion had begun also scarcely suppressed the brain damage. Taken together, these data indicate that the therapeutic time window for FK506-liposomes was up to 2 h after MCAO/reperfusion in this experimental model rat, and suggest that the injection of them at an early time would result in a good outcome.

The motor ability of the t-MCAO rats was evaluated based on the 21-point motor score (Fig. 7). In the control group, hemiparesis was observed at 24 h after the start of reperfusion, resulting in a low score. On the other hand, t-MCAO rats treated with FK506-liposomes showed alleviated hemiparesis, especially in their hind legs. This recovery probably contributed to the high scores on the inclined platform test, horizontal bar test (forepaws placed on ribbed bar), and circling test obtained for the FK506-liposome-treated animals (Supplemental Table S1). The administration of free FK506 at 300  $\mu$ g/kg also significantly improved motor function deficit. These results correlated well with the extent of cerebral cell death and swelling.

## DISCUSSION

The present study showed that FK506-liposomes significantly suppressed neutrophil invasion and apoptotic cell death, and ameliorated neurological deficits in t-MCAO rats compared with free FK506. The liposomalization of FK506 might lead to an increase in the amount of drug accumulation in I/R regions. The disruption of blood-brain barrier is induced at an early



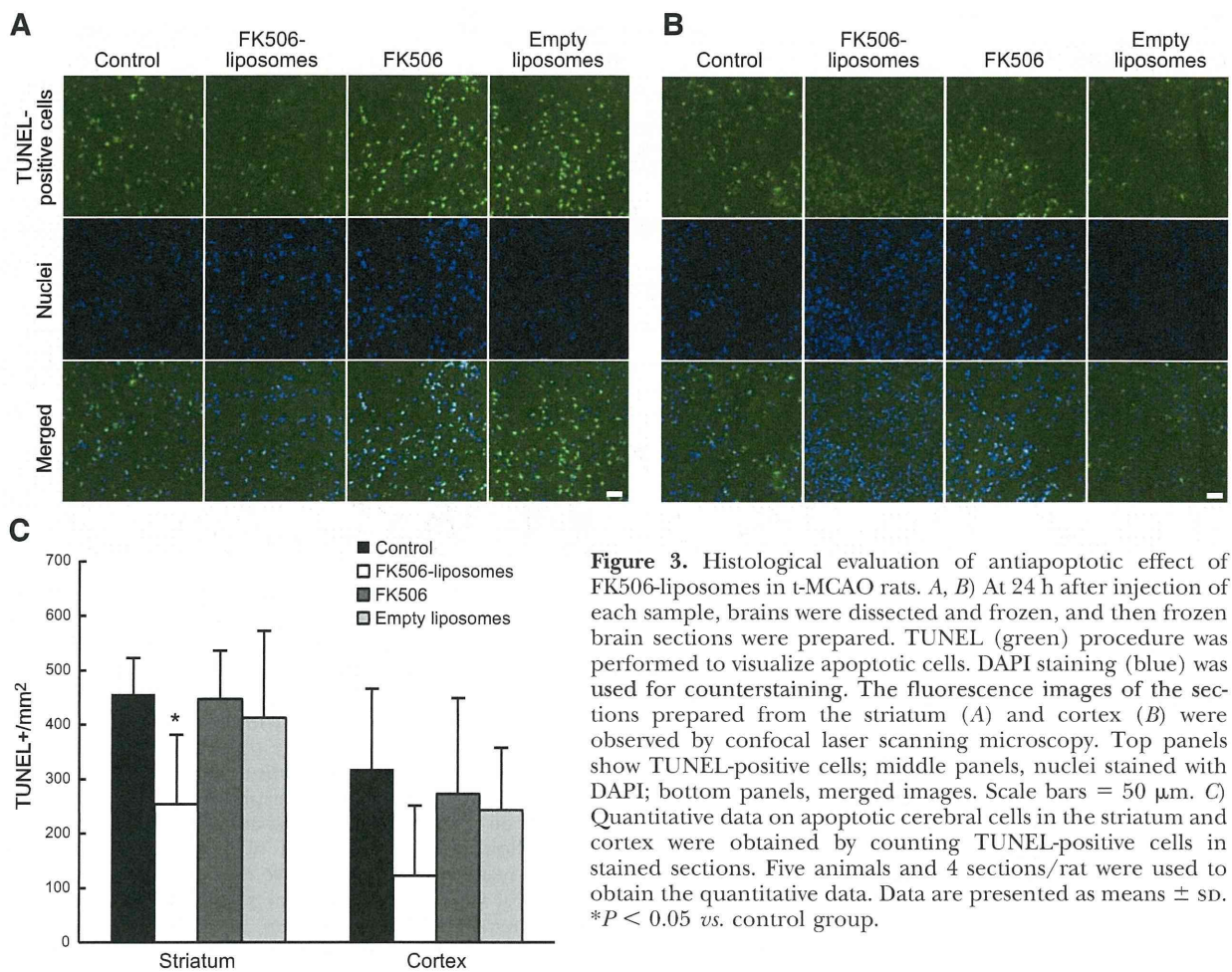


**Figure 3.** Histological evaluation of antiapoptotic effect of FK506-liposomes in t-MCAO rats. *A, B*) At 24 h after injection of each sample, brains were dissected and frozen, and then frozen brain sections were prepared. TUNEL (green) procedure was performed to visualize apoptotic cells. DAPI staining (blue) was used for counterstaining. The fluorescence images of the sections prepared from the striatum (*A*) and cortex (*B*) were observed by confocal laser scanning microscopy. Top panels show TUNEL-positive cells; middle panels, nuclei stained with DAPI; bottom panels, merged images. Scale bars = 50  $\mu\text{m}$ . *C*) Quantitative data on apoptotic cerebral cells in the striatum and cortex were obtained by counting TUNEL-positive cells in stained sections. Five animals and 4 sections/rat were used to obtain the quantitative data. Data are presented as means  $\pm$  SD. \* $P < 0.05$  vs. control group.

stage in the ischemic core region after cerebral ischemia (19, 20). Moreover, a previous report demonstrated that the area in which macromolecules accumulate expands as time passes after I/R in t-MCAO rats (21). Hence, the concept of passive targeting, as constructed for cancer treatment, could be a promising

scheme for efficient drug delivery to I/R regions. In the present study, a higher extent of localization of FK506-liposomes in the ischemic hemisphere was observed at 24 h than at 3 h after the injection. This result suggests that the accumulation amount of FK506-liposomes given at the start of reperfusion gradually increased in

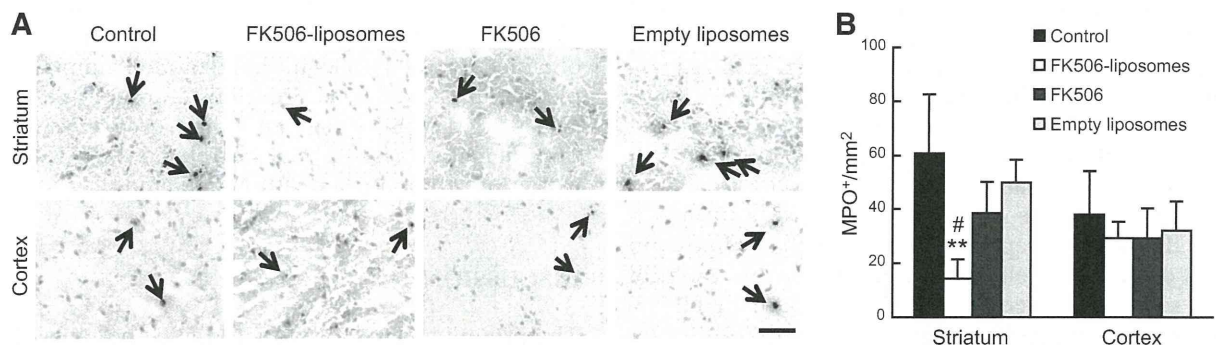


**Figure 4.** Invasion of neutrophils into the brain parenchyma of t-MCAO rats. At 24 h after injection of each sample, brains were dissected and frozen; and then frozen brain sections were prepared. MPO immunostaining was performed to visualize neutrophils (brown). Hematoxylin staining (blue) was used for counterstaining. *A*) Stained sections were observed by microscopy. Arrows indicate neutrophils that had infiltrated the brain parenchyma. Scale bar = 50  $\mu\text{m}$ . *B*) Quantitative data on neutrophil invasion analysis were obtained by counting MPO-positive cells in stained sections. Data are presented as means  $\pm$  SD ( $n=6$ ). \*\* $P < 0.01$  vs. control group; # $P < 0.05$  vs. free FK506-treated group.

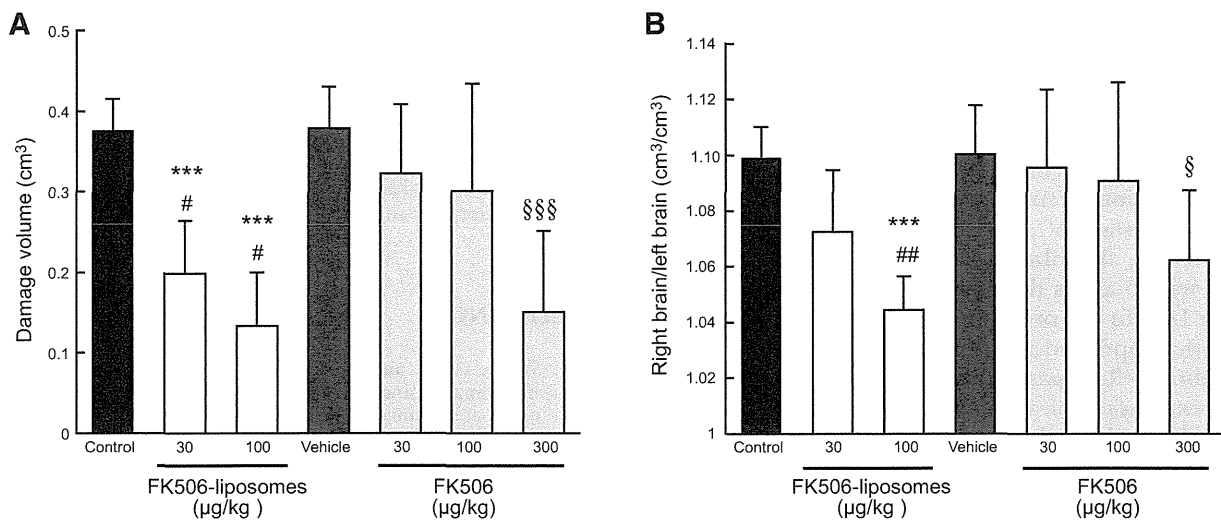


**Figure 5.** Suppression of cerebral cell death and brain swelling by the treatment with FK506-liposomes. t-MCAO rats were injected *via* a tail vein with PBS, FK506-liposomes, vehicle for free FK506 or free FK506 immediately after the start of reperfusion at dosages indicated as FK506. At 24 h after injection, brains were dissected and stained with TTC. Damage volume (A) and degree of brain swelling (B) were calculated by using Image J. Data are means  $\pm$  SD ( $n=7$ ). \*\*\* $P < 0.001$  vs. control group; # $P < 0.05$ , ## $P < 0.01$  vs. free FK506-treated group at the same dose; § $P < 0.05$ , §§§ $P < 0.001$  vs. vehicle-treated group.

a time-dependent manner, as in the case of enhanced permeability and retention effect. However, the half-life of free FK506 is extremely short, and FK506 administered intravenously is almost totally metabolized by the liver, primarily by cytochrome P450 3A (22, 23). The change in biodistribution afforded by liposomalization would be expected to be closely related to the therapeutic outcome.

Fatal damage in the striatum, the region assumed to be the ischemic core in the present experimental model, occurs at an early stage after an I/R event (21).

In this study, FK506-liposomes substantially reduced the cerebral cell death and inflammation induced by I/R in this region. Thus, FK506-liposomes spreading into the brain parenchyma quickly showed pharmacological activity. Although PEG-modification of liposomes prolongs their circulation in the blood, it causes a decrease in cellular uptake of liposomes (24, 25). Therefore, FK506-liposomes reaching I/R regions might have released FK506 into the brain parenchyma, and the released drugs then acted on the cerebral cells.

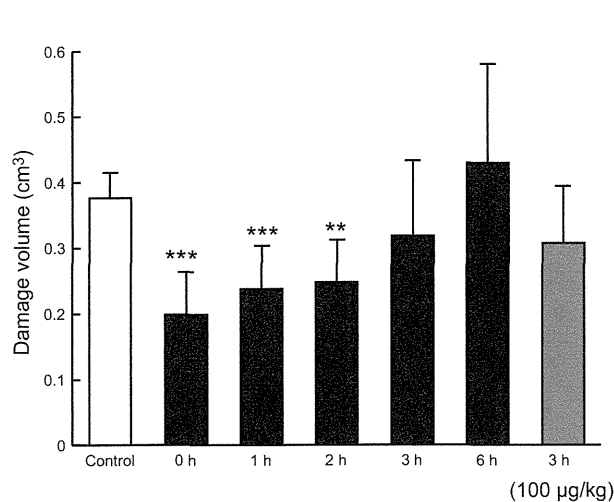


**Figure 6.** Therapeutic time window of FK506-liposomes in t-MCAO rats. t-MCAO rats were intravenously injected *via* a tail vein with FK506-liposomes (30 or 100  $\mu\text{g}/\text{kg}$  as FK506 dosage) at the indicated times (0, 1, 2, 3, or 6 h) after the start of reperfusion. At 24 h after reperfusion had begun, brain was dissected and stained with TTC. Damage volume was calculated by using Image J. Data are presented as means  $\pm$  SD ( $n=6-7$ ). \*\* $P < 0.01$ , \*\*\* $P < 0.001$  vs. control.

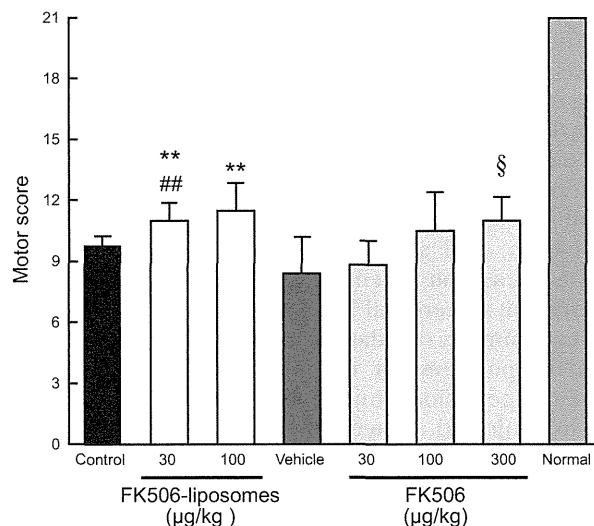


**Figure 7.** Motor activity score of t-MCAO rats. t-MCAO rats were treated with each sample as described in the legend of Fig. 5, and these rats were then assessed for motor function in a 21-point neuropathological scoring system. Data are presented as means  $\pm$  SD ( $n=7$ ). \*\* $P < 0.01$  vs. control group; ## $P < 0.01$  vs. free FK506-treated group at the same dose; § $P < 0.05$  vs. vehicle-treated group.



Neutrophils generate cytotoxic substances such as hypochlorous acid in inflammation sites, resulting in progressive inflammation. These cells normally do not exist in the brain, but they do invade into the cerebral parenchyma *via* brain endothelial cells after a cerebral ischemic event. This invasion induced by intracerebral inflammation occurs during the period of 9 to 24 h after the start of reperfusion in t-MCAO rats (26). Therefore, the observation of neutrophil invasion is one way to assess the extent of cerebral inflammation after I/R. In the present study, FK506-liposomes significantly suppressed the neutrophil invasion induced by cerebral I/R. A past study showed that FK506 inhibits the expression of adhesion molecules in the cerebral vasculature by reducing the production of inflammatory cytokines by neuronal cells and glia cells (26). Accordingly, we suggest that FK506-liposomes administered after the start of reperfusion inhibited the inflammatory response by affecting neuronal cells and glia cells in the t-MCAO rats.

FK506 directly suppresses apoptotic cell death induced by cerebral I/R through the inhibition of Bad dephosphorylation and subsequent cytochrome *c* release (27, 28). In addition, the prevention of reactive oxygen species production is related to its antiapoptotic effect on cerebral cells injured by I/R (29). The present study demonstrated that FK506-liposomes markedly reduced the number of apoptotic cells in t-MCAO rats. These multifunctional mechanisms, including the anti-inflammatory effect of FK506-liposomes, probably effectively acted on the neurovascular unit to bring about the good outcome in the t-MCAO rats.

A large number of small molecules as neuroprotectants have failed in clinical trials (30). Based on our present data, we propose that liposomalization of small molecular neuroprotectants should overcome their insufficiency of medicinal efficacy and adverse side effects. Liposomes can encapsulate many kinds of drugs regardless of their being hydrophilic or hydrophobic. Furthermore, liposomes can be modified with functional molecules, resulting in improved biodistribution, controlled release of drugs, increase in drug accumulation in targeted cells, regulation of intracellular distribution, and so on (31–34). Therefore, liposomal DDS has a great potential to be a novel strategy for the treatment of cerebral I/R injury.

In summary, our data demonstrate the usefulness of FK506-liposomes for the treatment of cerebral ischemia/reperfusion injury. FK506-liposomes intravenously injected immediately after the start of reperfusion significantly suppressed neutrophil invasion, apoptotic cell death, and infarct volume compared with free FK506 in t-MCAO rats. In addition, the motor function deficits induced by ischemia/reperfusion in these rats were ameliorated to a greater extent by the treatment with FK506-liposomes than by that with free FK506. Therefore, liposomalization of FK506 should permit a reduction in the dosage of FK506 without a decrease in the therapeutic efficacy of the drug. Taken together, our present findings indicate

that FK506-liposomes have a clear potential to be a neuroprotectant if administered quickly after a cerebral stroke. F

The authors thank Astellas Pharmaceutical Co., Ltd. (Tokyo, Japan) for the gift of the FK506. This research was supported by a grant-in-aid for scientific research from the Japan Society for the Promotion of Science.

## REFERENCES

- Wong, C. H., and Crack, P. J. (2008) Modulation of neuroinflammation and vascular response by oxidative stress following cerebral ischemia-reperfusion injury. *Curr. Med. Chem.* **15**, 1–14
- Eltzschig, H. K., and Eckle, T. (2011) Ischemia and reperfusion—from mechanism to translation. *Nat. Med.* **17**, 1391–1401
- Tuma, R. F., and Steffens, S. (2012) Targeting the endocannabinoid system to limit myocardial and cerebral ischemic and reperfusion injury. *Curr. Pharm. Biotechnol.* **13**, 46–58
- Ginsberg, M. D. (2009) Current status of neuroprotection for cerebral ischemia: synaptic overview. *Stroke* **40**, S111–114
- Ishii, T., Asai, T., Oyama, D., Fukuta, T., Yasuda, N., Shimizu, K., Minamino, T., and Oku, N. (2012) Amelioration of cerebral ischemia-reperfusion injury based on liposomal drug delivery system with asialo-erythropoietin. *J. Control. Release* **160**, 81–87
- Sharkey, J., and Butcher, S. P. (1994) Immunophilins mediate the neuroprotective effects of FK506 in focal cerebral ischaemia. *Nature* **371**, 336–339
- Furuichi, Y., Maeda, M., Moriguchi, A., Sawamoto, T., Kawamura, A., Matsuoka, N., Mutoh, S., and Yanagihara, T. (2003) Tacrolimus, a potential neuroprotective agent, ameliorates ischemic brain damage and neurologic deficits after focal cerebral ischemia in nonhuman primates. *J. Cereb. Blood Flow Metab.* **23**, 1183–1194
- Szydłowska, K., Zawadzka, M., and Kaminska, B. (2006) Neuroprotectant FK506 inhibits glutamate-induced apoptosis of astrocytes in vitro and in vivo. *J. Neurochem.* **99**, 965–975
- Morioka, M., Hamada, J., Ushio, Y., and Miyamoto, E. (1999) Potential role of calcineurin for brain ischemia and traumatic injury. *Prog. Neurobiol.* **58**, 1–30
- Wang, H. G., Pathan, N., Ethell, I. M., Krajewski, S., Yamaguchi, Y., Shibasaki, F., McKeon, F., Bobo, T., Franke, T. F., and Reed, J. C. (1999) Ca<sup>2+</sup>-induced apoptosis through calcineurin dephosphorylation of BAD. *Science* **284**, 339–343
- Hashiguchi, A., Kawano, T., Yano, S., Morioka, M., Hamada, J., Sato, T., Shirasaki, Y., Ushio, Y., and Fukunaga, K. (2003) The neuroprotective effect of a novel calmodulin antagonist, 3-[2-[4-(3-chloro-2-methylphenyl)-1-piperazinyl]ethyl]-5,6-dimethoxy-1-(4-imidazolylmethyl)-1H-indazole dihydrochloride 3.5 hydrate, in transient forebrain ischemia. *Neuroscience* **121**, 379–386
- Kaminska, B., Gaweda-Walerych, K., and Zawadzka, M. (2004) Molecular mechanisms of neuroprotective action of immunosuppressants—facts and hypotheses. *J. Cell. Mol. Med.* **8**, 45–58
- Chuang, Y. C., Tyagi, P., Huang, H. Y., Yoshimura, N., Wu, M., Kaufman, J., and Chancellor, M. B. (2011) Intravesical immune suppression by liposomal tacrolimus in cyclophosphamide-induced inflammatory cystitis. *Neurourol. Urodyn.* **30**, 421–427
- Moffatt, S. D., McAlister, V., Calne, R. Y., and Metcalfe, S. M. (1999) Potential for improved therapeutic index of FK506 in liposomal formulation demonstrated in a mouse cardiac allograft model. *Transplantation* **67**, 1205–1208
- Longa, E. Z., Weinstein, P. R., Carlson, S., and Cummins, R. (1989) Reversible middle cerebral artery occlusion without craniectomy in rats. *Stroke* **20**, 84–91
- Zhang, N., Komine-Kobayashi, M., Tanaka, R., Liu, M., Mizuno, Y., and Urabe, T. (2005) Edaravone reduces early accumulation of oxidative products and sequential inflammatory responses after transient focal ischemia in mice brain. *Stroke* **36**, 2220–2225
- Toung, T. J., Bhardwaj, A., Dawson, V. L., Dawson, T. M., Traystman, R. J., and Hurn, P. D. (1999) Neuroprotective FK506 does not alter in vivo nitric oxide production during ischemia and early reperfusion in rats. *Stroke* **30**, 1279–1285

18. Hunter, A. J., Hatcher, J., Virley, D., Nelson, P., Irving, E., Hadingham, S. J., and Parsons, A. A. (2000) Functional assessments in mice and rats after focal stroke. *Neuropharmacology* **39**, 806–816
19. Rosenberg, G. A., Estrada, E. Y., and Dencoff, J. E. (1998) Matrix metalloproteinases and TIMPs are associated with blood-brain barrier opening after reperfusion in rat brain. *Stroke* **29**, 2189–2195
20. Dirnagl, U., Iadecola, C., and Moskowitz, M. A. (1999) Pathobiology of ischaemic stroke: an integrated view. *Trends Neurosci.* **22**, 391–397
21. Ishii, T., Asai, T., Urakami, T., and Oku, N. (2010) Accumulation of macromolecules in brain parenchyma in acute phase of cerebral infarction/reperfusion. *Brain Res.* **1321**, 164–168
22. Yura, H., Yoshimura, N., Hamashima, T., Akamatsu, K., Nishikawa, M., Takakura, Y., and Hashida, M. (1999) Synthesis and pharmacokinetics of a novel macromolecular prodrug of Tacrolimus (FK506), FK506-dextran conjugate. *J. Control. Release* **57**, 87–99
23. Shiraga, T., Matsuda, H., Nagase, K., Iwasaki, K., Noda, K., Yamazaki, H., Shimada, T., and Funae, Y. (1994) Metabolism of FK506, a potent immunosuppressive agent, by cytochrome P450 3A enzymes in rat, dog and human liver microsomes. *Biochem. Pharmacol.* **47**, 727–735
24. Duzgune, scedil, and Nir, S. (1999) Mechanisms and kinetics of liposome-cell interactions. *Adv. Drug Deliv. Rev.* **40**, 3–18
25. Vertut-Doi, A., Ishiwata, H., and Miyajima, K. (1996) Binding and uptake of liposomes containing a poly(ethylene glycol) derivative of cholesterol (stealth liposomes) by the macrophage cell line J774: influence of PEG content and its molecular weight. *Biochim. Biophys. Acta* **1278**, 19–28
26. Noto, T., Furuichi, Y., Ishiye, M., Matsuoka, N., Aramori, I., Mutoh, S., and Yanagihara, T. (2007) Tacrolimus (FK506) limits accumulation of granulocytes and platelets and protects against brain damage after transient focal cerebral ischemia in rat. *Biol. Pharm. Bull.* **30**, 313–317
27. Li, J. Y., Furuichi, Y., Matsuoka, N., Mutoh, S., and Yanagihara, T. (2006) Tacrolimus (FK506) attenuates biphasic cytochrome c release and Bad phosphorylation following transient cerebral ischemia in mice. *Neuroscience* **142**, 789–797
28. Shichinohe, H., Kuroda, S., Abumiya, T., Ikeda, J., Kobayashi, T., Yoshimoto, T., and Iwasaki, Y. (2004) FK506 reduces infarct volume due to permanent focal cerebral ischemia by maintaining BAD turnover and inhibiting cytochrome c release. *Brain Res.* **1001**, 51–59
29. Dawson, T. M., Steiner, J. P., Dawson, V. L., Dinerman, J. L., Uhl, G. R., and Snyder, S. H. (1993) Immunosuppressant FK506 enhances phosphorylation of nitric oxide synthase and protects against glutamate neurotoxicity. *Proc. Natl. Acad. Sci. U.S.A.* **90**, 9808–9812
30. Sahota, P., and Savitz, S. I. (2011) Investigational therapies for ischemic stroke: neuroprotection and neurorecovery. *Neurotherapeutics* **8**, 434–451
31. Asai, T., Matsushita, S., Kenjo, E., Tsuzuku, T., Yonenaga, N., Koide, H., Hatanaka, K., Dewa, T., Nango, M., Maeda, N., Kikuchi, H., and Oku, N. (2011) Dicycyl phosphate-tetraethylenepentamine-based liposomes for systemic siRNA delivery. *Bioconjug. Chem.* **22**, 429–435
32. Tan, M. L., Choong, P. F., and Dass, C. R. (2010) Recent developments in liposomes, microparticles and nanoparticles for protein and peptide drug delivery. *Peptides* **31**, 184–193
33. Torres, E., Mainini, F., Napolitano, R., Fedeli, F., Cavalli, R., Aime, S., and Terreno, E. (2011) Improved paramagnetic liposomes for MRI visualization of pH triggered release. *J. Control. Release* **154**, 196–202
34. Micheli, M. R., Bova, R., Magini, A., Polidoro, M., and Emiliani, C. (2012) Lipid-based nanocarriers for CNS-targeted drug delivery. *Recent Pat. CNS Drug Discov.* **7**, 71–86

Received for publication October 1, 2012.  
Accepted for publication December 4, 2012.

# Liposomal Amiodarone Augments Anti-arrhythmic Effects and Reduces Hemodynamic Adverse Effects in an Ischemia/Reperfusion Rat Model

Hiroyuki Takahama · Hirokazu Shigematsu · Tomohiro Asai · Takashi Matsuzaki · Shoji Sanada · Hai Ying Fu · Keiji Okuda · Masaki Yamato · Hiroshi Asanuma · Yoshihiro Asano · Masanori Asakura · Naoto Oku · Issei Komuro · Masafumi Kitakaze · Tetsuo Minamino

Published online: 24 January 2013  
© Springer Science+Business Media New York 2013

## Abstract

**Purpose** Although amiodarone is recognized as the most effective anti-arrhythmic drug available, it has negative hemodynamic effects. Nano-sized liposomes can accumulate in and selectively deliver drugs to ischemic/reperfused (I/R) myocardium, which may augment drug effects and reduce side effects. We investigated the effects of liposomal amiodarone on lethal arrhythmias and hemodynamic parameters in an ischemia/reperfusion rat model.

**Methods and Results** We prepared liposomal amiodarone (mean diameter:  $113 \pm 8$  nm) by a thin-film method. The left coronary artery of experimental rats was occluded for 5 min followed by reperfusion. Ex vivo fluorescent imaging revealed

that intravenously administered fluorescent-labeled nano-sized beads accumulated in the I/R myocardium. Amiodarone was measurable in samples from the I/R myocardium when liposomal amiodarone, but not amiodarone, was administered. Although the intravenous administration of amiodarone (3 mg/kg) or liposomal amiodarone (3 mg/kg) reduced heart rate and systolic blood pressure compared with saline, the decrease in heart rate or systolic blood pressure caused by liposomal amiodarone was smaller compared with a corresponding dose of free amiodarone. The intravenous administration of liposomal amiodarone (3 mg/kg), but not free amiodarone (3 mg/kg), 5 min before ischemia showed a significantly reduced duration of lethal arrhythmias ( $18 \pm 9$  s) and mortality (0 %) during the reperfusion period compared with saline ( $195 \pm 42$  s, 71 %, respectively).

**Conclusions** Targeting the delivery of liposomal amiodarone to ischemic/reperfused myocardium reduces the mortality due to lethal arrhythmia and the negative hemodynamic changes caused by amiodarone. Nano-size liposomes may be a promising drug delivery system for targeting I/R myocardium with cardioprotective agents.

T. Matsuzaki · S. Sanada · H. Y. Fu · K. Okuda · M. Yamato · Y. Asano · I. Komuro · T. Minamino (✉)  
Department of Cardiovascular Medicine, Osaka University Graduate School of Medicine, 2-2 Yamadaoka, Suita, Osaka 565-0871, Japan  
e-mail: minamino@cardiology.med.osaka-u.ac.jp

H. Takahama · M. Asakura · M. Kitakaze  
Department of Cardiovascular Medicine, National Cerebral and Cardiovascular Center, Suita 565-8565, Japan

H. Shigematsu · T. Asai · N. Oku  
Department of Medical Biochemistry and Global COE, University of Shizuoka Graduate School of Pharmaceutical Sciences, Shizuoka 422-8526 Shizuoka, Japan

H. Asanuma  
Department of Cardiovascular Science and Technology, Kyoto Prefectural University School of Medicine, Kyoto 602-8566, Japan

H. Takahama  
Division of Cardiovascular Disease, Mayo Clinic, Rochester, MN 55902, USA

**Keywords** Liposome · Amiodarone · Lethal arrhythmia · Ischemia · Reperfusion

## Introduction

Therapies for the prevention and treatment of ischemia-induced life-threatening arrhythmias remain an unmet medical need [1]. Amiodarone is currently considered to be the most effective anti-arrhythmic drug available for treating life-threatening arrhythmias [2, 3], despite the fact that this compound has a negative impact on hemodynamic parameters [4, 5]. The intravenous administration of amiodarone is expected

to be beneficial for the immediate treatment of arrhythmias in emergency settings, such as acute myocardial infarction (AMI) [6, 7]. However, in clinical practice, the administration of amiodarone remains problematic for the treatment of AMI [8]. Although lower doses of amiodarone result in fewer incidences of death, high doses of amiodarone can cause hypotension and non-cardiac death, both of which may diminish the positive effects of amiodarone [8, 9]. Therefore, a novel delivery system is strongly desired to enhance the anti-arrhythmic effects of amiodarone without producing severe side effects.

Liposomes are widely used for drug delivery to actively or passively target specific organs and to improve drug stability in cancer and inflammatory diseases [10–12]. In ischemic/reperfused (I/R) myocardium, cellular permeability is enhanced and vascular endothelial integrity is disrupted [13, 14], suggesting that nanoparticles, such as liposomes, may be a promising drug delivery system for targeting I/R myocardium with cardioprotective agents [15]. Indeed, we have recently demonstrated that adenosine encapsulated by liposomes coated with polyethylene glycol (PEG) exhibited enhanced cardioprotective effects and attenuated side effects, such as hypotension and bradycardia, in an ischemia/reperfusion model of rats [16]. In the present study, we prepared liposomal amiodarone and examined 1) the targeted accumulation of liposomal amiodarone in the I/R myocardium, 2) the hemodynamic effects of the intravenous administration of liposomal amiodarone and free amiodarone, and 3) the anti-arrhythmic effects of these preparations in an I/R rat model. We showed that targeting the delivery of liposomal amiodarone to I/R myocardium reduces the mortality due to lethal arrhythmias and the negative hemodynamic changes caused by amiodarone in an I/R rat model.

## Methods

### Materials

The materials used to prepare PEGylated liposomes, including 1-palmitoyl-2-oleoyl-sn-glycero-3-phosphocholine (POPC), 1,2-dipalmitoyl-sn-glycero-3-phosphocholine (DPPC), cholesterol, and 1,2-distearoyl-sn-glycero-3-phosphoethanolamine-N-poly(ethylene glycol) 2000 (DSPE-PEG2000), were kindly donated by Nippon Fine Chemical Co. (Taka-sago, Hyogo, Japan). Fluorescent beads (diameter 100 nm) were purchased from Invitrogen. All other materials were obtained from Sigma-Aldrich (St. Louis, MO, USA).

### Animals

Male Wistar rats (9 weeks old and weighing 250–310 g; Japan Animals, Osaka, Japan) were used. The animal experiments were approved by the Osaka University Research Committee

and were performed according to institutional guidelines. All studies conformed to the Guide for the care and Use of Laboratory Animals published by the US National Institutes of Health (NIH Publication No. 85–23, revised 1996).

### Preparation of PEGylated Liposomes

PEGylated liposomes composed of POPC, DPPC, cholesterol, DSPE-PEG2000, and amiodarone were prepared by a thin-film method. Briefly, amiodarone and lipids dissolved in chloroform were evaporated to form a thin lipid film using a rotary evaporator. The lipid film was dried for at least 1 h under reduced pressure and then hydrated with PBS (pH7.4). The liposome solution was freeze-thawed for 3 cycles with liquid nitrogen. The particle size of the liposomes was adjusted by extrusion through 100-nm-pore polycarbonate filters (Nuclepore, Cambridge, MA, USA). The liposomal solutions were centrifuged at 453,000 g for 15 min (CS120GXL, Hitachi, Japan) to remove the untrapped amiodarone. Then, the liposomes were resuspended in PBS. To determine the efficacy of trapping amiodarone in the liposomes, an aliquot of the liposomal solution was solubilized with 1 % reduced Triton X-100 (Sigma-Aldrich), and the amount of amiodarone was optically determined at 240 nm.

### Characterization of PEGylated Liposomes

The particle size and  $\zeta$  potential of PEGylated liposomes diluted with PBS were measured by dynamic scatter analysis (Zetasizer Nano ZS; Malvern, Worcestershire, UK). The analyses were performed 15 times per sample, and the results represent the analysis of 3 independent experiments.

### Experimental Protocol

#### *Targeted Delivery of Fluorescent-labeled Nano-sized Beads to the I/R Myocardium*

The rats were anesthetized with intraperitoneal sodium pentobarbital (50 mg/kg). Catheters were advanced into the femoral vein to infuse the drugs. Ischemia/reperfusion was induced by 5 min of left coronary artery occlusion followed by reperfusion [16]. After the hemodynamic parameters became stable, fluorescent-labeled nano-size beads, 100 nm in diameter (FluoSpheres, Invitrogen), were intravenously infused to the rats for 5 min before ischemia or before a sham operation ( $n=3$ , each). Fifteen minutes after reperfusion, the hearts were removed and cut into 5 sections parallel to the axis from the base to the apex. Then, ex vivo fluorescence images were obtained with an Olympus SZX12 stereoscopic microscope equipped with a DP71 digital camera (Olympus, Tokyo, Japan) before and after the hearts were sliced.



### *Targeted Delivery of Amiodarone and Liposomal Amiodarone to the I/R Myocardium*

Catheters were advanced into the femoral artery and vein to measure the systemic blood pressure (BP) and to infuse the drugs into the anesthetized rats, respectively. Electrocardiographic and hemodynamic parameters, such as heart rate (HR) and BP, were continuously monitored during the study using a PowerLab system (ADInstruments, Castle Hill, Australia). After the hemodynamic parameters became stable, to clarify the targeted delivery of amiodarone and liposomal amiodarone to the I/R myocardium, we intravenously administered saline, free amiodarone (3 mg/kg) or liposomal amiodarone (3 mg/kg) to rats for 5 min before the onset of ischemia. Then, we obtained blood samples and myocardium from the I/R area.

### *Effects of Amiodarone and Liposomal Amiodarone on Lethal Arrhythmias*

To evaluate the effects of amiodarone and liposomal amiodarone on lethal arrhythmias, we intravenously administered saline ( $n=7$ ), free amiodarone (3.0 or 10.0 mg/kg) ( $n=6$  each), PEGylated liposomes (empty liposomes) ( $n=6$ ), and PEGylated liposomal amiodarone (3.0 mg/kg) ( $n=6$ ) for 5 min before ischemia. The dose of amiodarone used in this study was lower than that used in a previous study [17] to clarify whether amiodarone encapsulated by liposomes coated with PEG exhibited enhanced anti-arrhythmic effects. Without any procedure such as electrical conversion or cardiac massage, ventricular tachyarrhythmias (VT/VF) occurred frequently during early period of reperfusion and the mortality of rats reached more than a half of cases in this model [18].

### *Measurement of Amiodarone Concentration*

The concentration of amiodarone in serum and heart tissue from the I/R area was assayed by high-performance liquid chromatography (HPLC) as previously described [19]. The detection limit of the HPLC assay was 50 ng/mL. Blood and myocardial samples were obtained at the end of the experimental protocol. The sample preparation was performed as previously described [19]. Briefly, myocardium was freed from visible blood, thereafter rinsed with 0.9 % sodium chloride and stored at  $-20^{\circ}\text{C}$  until analysis. After that, myocardial tissue samples were finely minced and 100 mg were homogenized with 0.9 % sodium chloride (1 mL) and after centrifugation, the clear supernatant was injected into HPLC.

### *Quantitative Evaluation of Fluorescent-labeled Nano-sized Beads in the I/R Myocardium*

To analyze the quantitative fluorescent intensity, signals from heart slices were quantified by image analysis (Image

J; National Institutes of Health, USA) as previously described [20]. The signal intensity from the heart slices was evaluated as the average signals of the whole heart and the left ventricle (LV) (Fig. 2c).

### *Arrhythmia Analysis*

The electrocardiographic tracings were independently analyzed by two of the authors, who were blinded to the treatment assignment. The duration of each spontaneous ventricular tachycardia or fibrillation episode during the I/R protocol was measured using the time scale provided by the recording software. Ventricular tachycardia was defined as 4 or more consecutive ventricular ectopic beats, and ventricular fibrillation was defined as a signal in which the individual QRS deflections could not easily be distinguished from one another. However, distinguishing ventricular tachycardia from fibrillation was often difficult [21]; therefore, we report ventricular tachycardia and fibrillation collectively as ventricular tachyarrhythmias (VT/VF) in this study. VT/VF duration and mortality were evaluated for 5 min of ischemia followed by 15 min of reperfusion.

### *Statistical Analysis*

The parameters of the liposomes are expressed as the mean  $\pm$  standard deviation (SD). Other data are expressed as the average  $\pm$  standard error of the mean (SEM). To compare the parameters of the liposomes, unpaired *t*-tests were performed. We performed the Welch *t*-test to compare the amiodarone concentration in the plasma and myocardium. For hemodynamic parameters, the data were assessed with the paired *t*-test for comparisons to the baseline within a group. One-way repeated-measurement ANOVA followed by post-hoc Bonferroni's multiple comparisons were used for comparisons between groups. To address the differences in VT/VF duration among the groups, we performed a non-parametric (Kruskal-Wallis) test followed by evaluation with the Mann-Whitney *U* test. The mortality rates were compared using the Fisher's exact probability test. In all analyses,  $P<0.05$  was considered to be statistically significant.

## **Results**

### *Characterization of PEGylated Liposomes*

We prepared 5 types of PEGylated liposomes composed of POPC, DPPC, cholesterol, and amiodarone. The ratio of unsaturated lipids (POPC) to saturated lipids (DPPC) varied (Fig. 1). During preparation of the liposomes, the POPC:DPPC:cholesterol:amiodarone molar ratio of 10:0:5:1 exhibited the best encapsulation efficiency for amiodarone compared with the other conditions (Fig. 1).

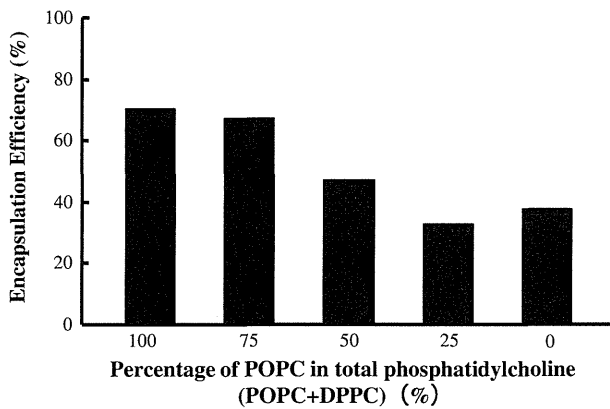


**Fig. 1** Encapsulation efficiency of amiodarone in the liposomes. Amiodarone was loaded into liposomes containing POPC, DPPC, or a mixture of POPC and DPPC. The liposomal amiodarone was composed of phosphatidylcholine (POPC + DPPC):cholesterol:amiodarone at a 10:5:1 molar ratio. The percent molar ratio of POPC in total phosphatidylcholine (POPC + DPPC) is indicated in the figure. The encapsulation efficiency of amiodarone was determined as described in the Methods section

The dynamic light scatter analysis showed no significant differences between the mean diameter, polydispersity index, or  $\zeta$  potential distribution of the empty and amiodarone-loaded PEGylated liposomes (Table 1).

#### Accumulation of Fluorescence-labeled Nano-sized Beads in the I/R Myocardium

Representative pictures obtained by fluorescence imaging are shown in Fig. 2a (whole heart) and b (sliced hearts). Quantitative analysis revealed that the average fluorescence intensity of the whole heart (Fig. 2c left) or the left ventricle (Fig. 2c right) of the I/R hearts was significantly higher than that in sham-operated hearts.

#### Amiodarone Concentration in the Blood and I/R Myocardium

The plasma concentration after the administration of liposomal amiodarone was significantly higher than that of free amiodarone (Table 2). Importantly, the amiodarone concentration in the I/R myocardium was detectable after the administration of liposomal, but not free, amiodarone (Table 2).

**Table 1** Characterization of liposomes by dynamic light scatter analysis

	Mean diameter (nm)	Polydispersity index	$\zeta$ Potential (mV)
PEGylated liposomes (empty liposomes)	111±14	0.124±0.027	-2.1
PEGylated liposomal amiodarone	113±8	0.128±0.040	-3.7

Results represent 4 independent experiments. The values are expressed as the mean ± SD. PEG polyethylene glycol

#### Hemodynamic Effects of Amiodarone and Liposomal Amiodarone

The baseline heart rates were  $411\pm 16$ ,  $426\pm 14$ ,  $427\pm 12$ ,  $409\pm 8$  and  $414\pm 6$  beats/min in the saline, empty liposome, amiodarone (3 mg/kg), amiodarone (10 mg/kg) and liposomal amiodarone (3 mg/kg) groups, respectively. The baseline systolic BP was  $113\pm 7$ ,  $118\pm 10$ ,  $111\pm 5$ ,  $90\pm 4$  and  $104\pm 2$  mmHg in the saline, empty liposome, amiodarone (3 mg/kg), amiodarone (10 mg/kg) and liposomal amiodarone (3 mg/kg) groups, respectively. There were no significant differences in the baseline HR or systolic BP among the groups tested. The intravenous administration of amiodarone (3 and 10 mg/kg) or liposomal amiodarone reduced both the HR and systolic BP from the baseline, whereas the saline or empty liposomes did not (Fig. 3). The time-course changes of both the HR and systolic BP were significantly smaller in the liposomal amiodarone group (3 mg/kg) compared with the corresponding dose in the free amiodarone group (3 mg/kg) (Fig. 3). The reductions in HR and systolic BP at 1, but not 3, minutes after liposomal amiodarone administration were significantly smaller compared with those following the corresponding dose of amiodarone.

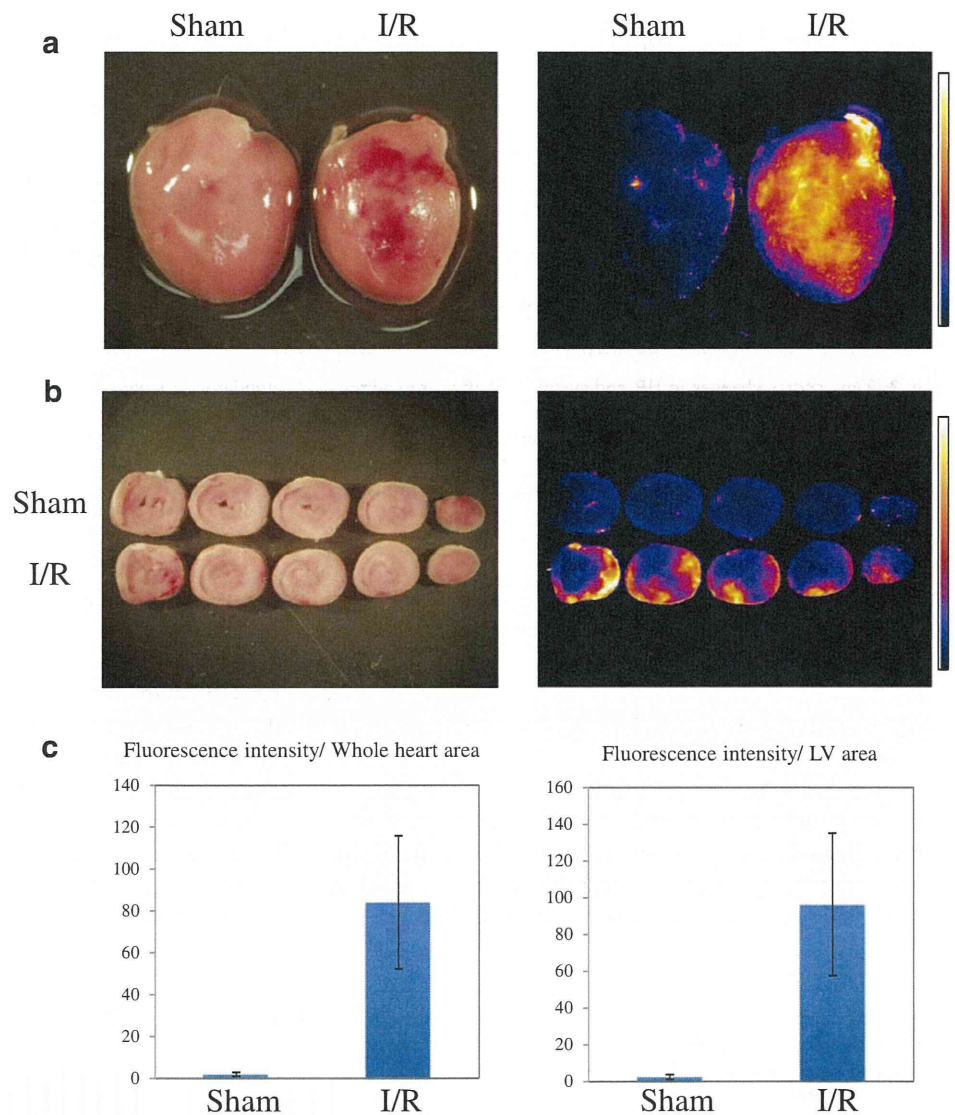
#### Antiarrhythmic Effects of Amiodarone and Liposomal Amiodarone

Representative electrocardiograms of the rats that received saline, free amiodarone or liposomal amiodarone are shown in Fig. 4. The intravenous administration of liposomal amiodarone (3 mg/kg), but not amiodarone (3 mg/kg), significantly reduced the duration of VT/VF compared with saline (Table 3). Furthermore, the mortality in the group that received liposomal amiodarone (3 mg/kg), but not the corresponding dose of amiodarone (3 mg/kg), was significantly lower than that in the saline group. In the group of rats that received a high dose of amiodarone (10 mg/kg), the VT/VF duration was  $36\pm 12$  s, and none of the rats died (Table 3), which was similar to the low dose of liposomal amiodarone group (3 mg/kg).

#### Discussion

In this study, we revealed that 1) liposomal amiodarone was successfully prepared using a thin-film method, 2) the

**Fig. 2** Representative pictures of ischemia/reperfused myocardium with and without fluorescence-labeled nano-sized beads. Representative pictures obtained by fluorescent imaging are shown in **a** (*whole heart*) and **b** (*sliced hearts*). Quantitative analysis revealed that the average fluorescence intensity of the whole heart (**c left**) or the left ventricle (**c right**) of the I/R hearts was significantly higher than that of the sham-operated hearts



accumulation of nano-sized beads was observed in the I/R myocardium, 3) liposomal amiodarone showed a smaller reduction in the HR and systolic BP compared with free amiodarone, and 4) liposomal amiodarone, but not amiodarone, reduced the VT/VF duration and mortality during the reperfusion period compared with saline.

**Table 2** Amiodarone concentration in the blood and I/R myocardium

Groups	Plasma, ng/mL	Myocardium, ng/mL
Saline	N.D.	N.D.
Free amiodarone	472±147	N.D.
Liposomal amiodarone	3872±378*	71±7*

Data are expressed as the mean ± SEM. N.D. not detected. n=3 rats in each group. \* p<0.05 versus free amiodarone

### Preparation of Liposomal Amiodarone

This study is the first to encapsulate amiodarone in PEGylated liposomes, although it has been previously encapsulated in other liposomes [22] and micelles [23]. We demonstrated that lipid bilayers composed of unsaturated lipids are more suitable for encapsulating amiodarone in PEGylated liposomes compared with those composed of saturated lipids. PEGylated liposomes have a long circulating time in the bloodstream because PEG endows a steric barrier to liposomes, allowing them to avoid interactions with opsonins and cells of the mononuclear phagocytic system [24]. Thus, they have been used to increase drug stability, safety, and bioavailability in clinical applications. In this study, we found that a higher concentration of amiodarone was retained in the blood when we administered liposomal amiodarone compared with the administration of

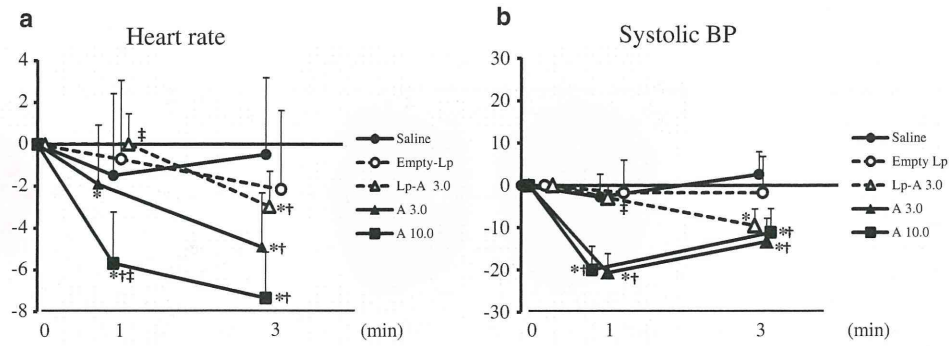


**Fig. 3** Time-course changes in HR and systolic BP after drug administration. Shows the percent change from baseline for HR (a) and systolic BP (b) after intravenous administration of the tested drugs. The data are expressed as the mean ± SEM. \* $P < 0.05$  versus baseline, paired  $t$ -test.  $P = 0.0009$  (HR),  $0.0002$  (systolic BP) between

amiodarone (3 mg/kg) and liposomal amiodarone (3 mg/kg), 1-way repeated-measurement ANOVA. † $P < 0.05$  versus saline, ‡ $P < 0.05$  versus amiodarone (3 mg/kg), 1-way repeated-measurement ANOVA with Bonferroni's multiple comparison

free amiodarone, suggesting that encapsulation of amiodarone in PEGylated liposomes enhances the stability of amiodarone in the blood.

#### Targeted Delivery to the I/R Myocardium by Liposomal Amiodarone

Ex vivo fluorescence imaging revealed that fluorescence-labeled nano-sized beads accumulated in the I/R myocardium, suggesting that myocardial permeability can be enhanced in the I/R myocardium. Consistent with this finding, we

observed that the amiodarone concentration in the I/R myocardium in the liposomal amiodarone group was much higher compared with that in the amiodarone group. Enhanced permeability in the I/R myocardium and the prolonged presence of amiodarone in PEGylated liposomes in the blood represent a possible mechanism for increased amiodarone concentrations in the I/R myocardium. Amiodarone will be released from accumulated liposomal amiodarone in I/R myocardium due to the natural decay and concentration gradient. These findings suggest that the I/R myocardium is a promising passive target for liposomal drug delivery.

**Fig. 4** Representative electrocardiograms. The upper, middle and lower panels show representative electrocardiograms under baseline conditions during ischemia and at the onset of reperfusion for rats that received saline, free amiodarone (3 mg/kg) and liposomal amiodarone (3 mg/kg), respectively

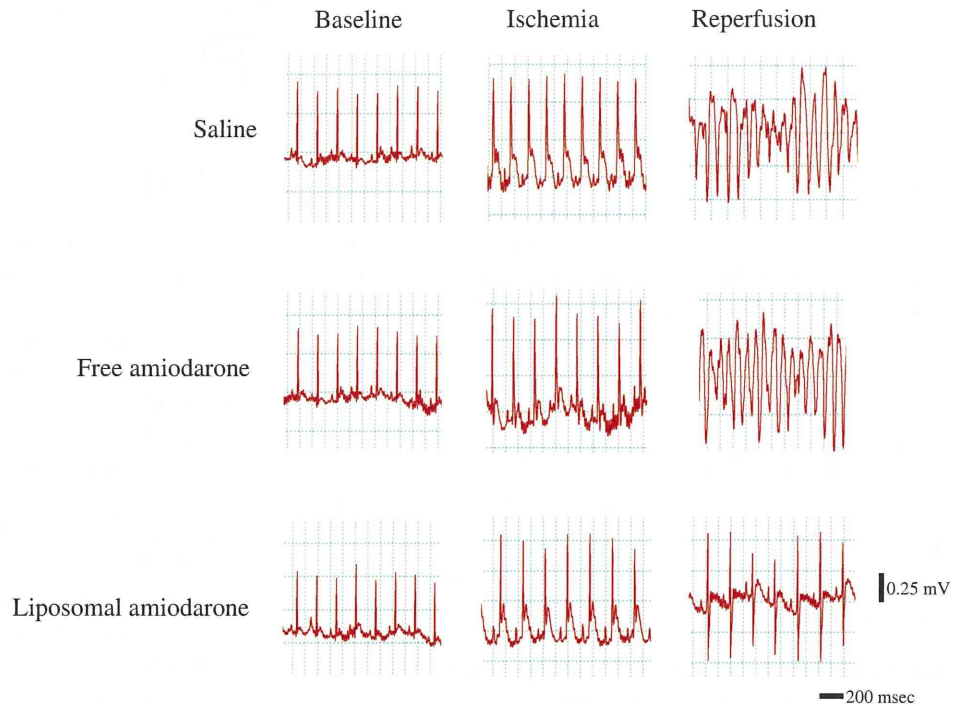




**Table 3** Lethal arrhythmias and mortality in an I/R rat model

	Number	VT/VF duration (sec)	Mortality (%)
Saline	7	195±42	71
Empty liposomes	6	162±31	50
Amiodarone (3 mg/kg)	6	167±78	33
Amiodarone (10 mg/kg)	6	36±12*	0#
Liposomal Amiodarone (3 mg/kg)	6	18±9*	0#

\* $p < 0.05$  versus saline (VT/VF duration). # $p < 0.05$  versus saline group (mortality). VT ventricular tachycardia, VF ventricular fibrillation

#### Minimal Negative Hemodynamic Effects of Liposomal Amiodarone

Amiodarone causes hypotension and bradycardia in clinical settings [4, 5]. In this study, both free and liposomal amiodarone significantly reduced the HR and systolic BP; however, the time-course changes for both the HR and systolic BP in the liposomal amiodarone group were significantly smaller compared with those following the corresponding dose of free amiodarone. Importantly, the reductions in HR and systolic BP at 1, but not 3, minutes after liposomal amiodarone administration were significantly smaller compared with those following the corresponding dose of amiodarone. These findings suggest that liposomal amiodarone may minimize the negative effects on systemic hemodynamics immediately after the administration of amiodarone. One possible mechanism to explain this finding is that amiodarone on the surface of the liposome membrane is covered with PEG so that amiodarone cannot act directly on cardiovascular cells. Gradual release of amiodarone from liposome may minimize the rapid hemodynamic changes, because systemic hemodynamic effects of liposomal amiodarone were significantly attenuated in liposomal amiodarone group than free amiodarone group.

#### Augmented Anti-arrhythmic Effects of Liposomal Amiodarone

In this study, liposomal amiodarone (3 mg/kg), but not the corresponding dose of free amiodarone (3 mg/kg), significantly reduced the VT/VF duration and mortality compared with saline in an I/R rat model. Because the acute effects of amiodarone are known to be attributable to blockade of  $\text{Na}^+$ ,  $\text{Ca}^{2+}$  and dose-dependent  $\text{K}^+$  channels [2, 25], increasing the concentration of amiodarone in the I/R myocardium may augment its anti-arrhythmic effects through its tonic effects on cardiomyocytes caused by blocking cardiac ionic currents. Kishida et al. reported that amiodarone enhances nitric oxide production in cultured human endothelial cells [26].

Furthermore, amiodarone protects cardiac myocytes against oxidative injury by scavenging free radicals [27]. These pleiotropic effects of amiodarone are also enhanced by its increased concentration in the I/R myocardium via PEGylated liposomes, which may contribute to the reduction of lethal arrhythmias during reperfusion followed by ischemia. In the present study, since we did not do any procedure such as electrical conversion or cardiac massage for VT/VF, the mortality was higher than in our previous report [16].

#### Clinical Implications

In clinical settings, higher doses of amiodarone cause hypotension and non-cardiac death or induce worsening heart failure through negative inotropic effects [28]. These effects often diminish the beneficial effects of amiodarone for patients with AMI or heart failure [8, 9]. The present study demonstrated that liposomal amiodarone (3 mg/kg) exerts anti-arrhythmic effects similar to a high dose of free amiodarone (10 mg/kg) while reducing the extent of bradycardia and hypotension, suggesting that encapsulating amiodarone in liposomes augments its anti-arrhythmic effects and reduces its negative effects on hemodynamic parameters with reducing administrative dose. These findings can have a great impact on preventing lethal arrhythmias during reperfusion in AMI patients.

#### Study Limitations

There are several limitations in this study. We used a brief period of I/R without myocardial infarction in rats. Sakamoto et al. demonstrated that the incidence of VT/VF in a rodent model was ‘bell-shaped’ with a maximum at 5 min of ischemia and that most lethal arrhythmias occurred within first 20 s after the onset of reperfusion [29]. Consistently, our data showed that the mean time at which the lethal arrhythmia occurred after the onset of reperfusion was  $3.3 \pm 1.6$  s. Therefore, we chose the 5 min of ischemia followed by 15 min of reperfusion model. We also chose the timing of drug administration before the onset of ischemia to clarify whether liposomal-amiodarone could prevent the lethal arrhythmia that occurs in the early period of reperfusion. In addition, in clinical practice lethal arrhythmias often occur after a brief period of I/R without any irreversible damage to the heart, indicating that the anti-arrhythmic effects of liposomal amiodarone during a brief period of ischemia model could have clinical relevance [30]. However, careful interpretation is necessary when using liposomal amiodarone in acute myocardial infarction with irreversible damage to confirm the beneficial effects of liposomal amiodarone. Furthermore, because the electrophysiology of rats differs from that of humans and drug administration in our study started before the onset of

ischemia, additional pre-clinical studies including a longer period of I/R model to consider the timing of drug administration are needed using large animal models. We should also take into account that the potential side effects of amiodarone such as bradycardia are minimal in the left coronary artery occlusion model used in the present study.

## Conclusion

In conclusion, the targeted delivery of liposomal amiodarone to the I/R myocardium exerted strong anti-arrhythmic effects and reduced the negative impact on systemic hemodynamics. Nano-sized liposomes may be a promising drug delivery system for targeting the I/R myocardium with cardioprotective agents.

**Acknowledgments** The authors thank Takaki Hayakawa for her technical assistance, Takeshi Aiba for his special advice about data analysis. This research was supported by Grants-in-Aid from the Ministry of Health, Labor, and Welfare of Japan; Grants-in-Aid from the Ministry of Education, Culture, Sports, Science, and Technology of Japan; grants from the Japan Heart Foundation; and grants from the Japan Cardiovascular Research Foundation.

## References

- Di Diego JM, Antzelevitch C. Ischemic ventricular arrhythmias: experimental models and their clinical relevance. *Hear Rhythm*. 2011;8:1963–8.
- Kodama I, Kamiya K, Toyama J. Cellular electropharmacology of amiodarone. *Cardiovasc Res*. 1997;35:13–29.
- Vassallo P, Trohman RG. Prescribing amiodarone: an evidence-based review of clinical indications. *JAMA*. 2007;298:1312–22.
- Scheinman MM, Levine JH, Cannom DS, et al. Dose-ranging study of intravenous amiodarone in patients life-threatening ventricular tachyarrhythmias. The Intravenous Amiodarone Multicenter Investigators Group. *Circulation*. 1995;92:3264–72.
- Podrid PJ. Amiodarone; reevaluation of an old drug. *Ann Intern Med*. 1995;122:689–700.
- Shiga T, Tanaka T, Irie S, Hagiwara N, Kasanuki H. Pharmacokinetics of intravenous amiodarone and its electrocardiographic effects on healthy Japanese subjects. *Hear Vessel*. 2011;26:274–81.
- Wenzel V, Russo SG, Arntz HR, et al. [Comments on the 2010 guidelines on cardiopulmonary resuscitation of the European Resuscitation Council.]. *Anaesthesist*. 2010.
- Elizari MV, Martínez JM, Belziti C, et al. Morbidity and mortality following early administration of amiodarone in acute myocardial infarction. GEMICA study investigators, GEMA Group, Buenos Aires, Argentina. Grupo de Estudios Multicentricos en Argentina. *Eur Heart J*. 2000;21:198–205.
- Hu K, Gaudron P, Ertl G. Effects of high- and low-dose amiodarone on mortality, left ventricular remodeling, and hemodynamics in rats with experimental myocardial infarction. *J Cardiovasc Pharmacol*. 2004;44:627–30.
- Semalty A, Semalty M, Rawat BS, Singh D, Rawat MS. Pharmacosomes: the lipid-based new drug delivery system. *Expert Opin Drug Deliv*. 2009;6:599–612.
- Whitehead KA, Langer R, Anderson DG. Knocking down barriers: advances in siRNA delivery. *Nat Rev Drug Discov*. 2009;8:129–38.
- Malam Y, Loizidou M, Seifalian AM. Liposomes and nanoparticles: nanosized vehicles for drug delivery in cancer. *Trends Pharmacol Sci*. 2009;30:592–9.
- Horwitz LD, Kaufman D, Keller MW, Kong Y. Time course of coronary endothelial healing after injury due to ischemia and reperfusion. *Circulation*. 1994;90:2439–47.
- Dauber IM, VanBenthuyzen KM, McMurtry IF, et al. Functional coronary microvascular injury evident as increased permeability due to brief ischemia and reperfusion. *Circ Res*. 1990;66:986–98.
- Galagudza MM, Korolev DV, Sonin DL, et al. Targeted drug delivery into reversibly injured myocardium with silica nanoparticles: surface functionalization, natural biodistribution, and acute toxicity. *Int J Nanomedicine*. 2010;5:231–7.
- Takahama H, Minamino T, Asanuma H, et al. Prolonged targeting of ischemic/reperfused myocardium by liposomal adenosine augments cardioprotection in rats. *J Am Coll Cardiol*. 2009;53:709–17.
- Riva E, Hearse DJ. Anti-arrhythmic effects of amiodarone and desethylamiodarone on malignant ventricular arrhythmias arising as a consequence of ischaemia and reperfusion in the anaesthetised rat. *Cardiovasc Res*. 1989;23:331–9.
- Canyon SJ, Dobson GP. Protection against ventricular arrhythmias and cardiac death using adenosine and lidocaine during regional ischemia in the in vivo rat. *Am J Physiol Heart Circ Physiol*. 2004;287:H1286–95.
- Plomp TA, Wiersinga WM, Maes RA. Tissue distribution of amiodarone and desethylamiodarone in rats after repeated oral administration of various amiodarone dosages. *Arzneimittelforschung*. 1985;35:1805–10.
- Feige JN, Sage D, Wahli W, Desvergne B, Gelman L. PixFRET, an ImageJ plug-in for FRET calculation that can accommodate variations in spectral bleed-throughs. *Microsc Res Tech*. 2005;68:51–8.
- Opitz CF, Mitchell GF, Pfeffer MA, Pfeffer JM. Arrhythmias and death after coronary artery occlusion in the rat. Continuous telemetric ECG monitoring in conscious, untethered rats. *Circulation*. 1995;92:253–61.
- Klibanov AL, Maruyama K, Torchilin VP, Huang L. Amphiphatic polyethyleneglycols effectively prolong the circulation time of liposomes. *FEBS Lett*. 1990;268:235–7.
- Theodossiou TA, Galanou MC, Paleos CM. Novel amiodarone-doxorubicin cocktail liposomes enhance doxorubicin retention and cytotoxicity in DU145 human prostate carcinoma cells. *J Med Chem*. 2008;51:6067–74.
- Elhasi S, Astaneh R, Lavasanifar A. Solubilization of an amphiphilic drug by poly(ethylene oxide)-block-poly(ester) micelles. *Eur J Pharm Biopharm*. 2007;65:406–13.
- Kamiya K, Nishiyama A, Yasui K, Hojo M, Sanguinetti MC, Kodama I. Short- and long-term effects of amiodarone on the two components of cardiac delayed rectifier K(+) current. *Circulation*. 2001;9:1317–24.
- Kishida S, Nakajima T, Ma J, et al. Amiodarone and N-desethylamiodarone enhance endothelial nitric oxide production in human endothelial cells. *Int Heart J*. 2006;47:85–93.
- Ide T, Tsutsui H, Kinugawa S, Utsumi H, Takeshita A. Amiodarone protects cardiac myocytes against oxidative injury by its free radical scavenging action. *Circulation*. 1999;100:690–2.
- Freedman MD, Somberg JC. Pharmacology and pharmacokinetics of amiodarone. *J Clin Pharmacol*. 1991;31:1061–9.
- Sakamoto J, Miura T, Tsuchida A, Fukuma T, Hasegawa T, Shimamoto K. Reperfusion arrhythmias in the murine heart: their characteristics and alteration after ischemic preconditioning. *Basic Res Cardiol*. 1999;94:489–95.
- Tzivoni D, Keren A, Granot H, Gottlieb S, Benhorin J, Stem S. Ventricular fibrillation caused by myocardial reperfusion in Prinzmetal's angina. *Am Heart J*. 1983;105:323–5.

